Heat and Mass Transfer accompanied by Crystallisation of single Particles containing Urea-water-solution

S. Kontin*, A. Höfler, R. Koch and H.-J. Bauer
Institut für Thermische Strömungsmaschinen
Karlsruhe Institute of Technology
D-76128 Karlsruhe, Germany

Abstract

The evaporation and decomposition of particles containing urea-water-solution (UWS) is investigated. An advanced model based on a well known film-model for single particles is proposed. Special emphasis is put on the oversaturation of evaporating UWS leading to precipitation and crystallisation of urea.

Introduction

For the Selective Catalytic Reduction (SCR) in today's DeNOx-systems UWS is sprayed into the hot exhaust gas of diesel engines. During the evaporation process, the water is removed from the particle and the remaining urea is then decomposed to the reducing agent ammonia [1]. An accurate model of the evaporation and decomposition of UWS is crucial for the prediction of the overall reduction process.

For studying the governing physicochemical process, single particle evaporating kinetics are investigated. Several authors reported about evaporating single particles over the last decades. In the pioneering experimental work by Frössling [2] the so called 'Windfaktor' was introduced. It describes the influence of a slip velocity between the particle and the continuous phase. Further research lead to enhanced numerical models describing the particle evaporation [3, 4].

The current status in the research about modelling sprays used for exhaust aftertreatment with SCR is given by Birkhold *et al.* [1]. In their work a Rapid Mixing (RM) model is applied for droplets containing UWS. The model is compared to a Diffusion Limit (DL) model and to an Effective Diffusion (ED) model. Despite resulting concentration gradients inside the droplet for the DL model, the particle size evolution agrees well between all models. The RM model is found to have the best trade-off between accuracy and numerical effort. However, the possible crystallisation of urea is neglected.

Previous experimental studies were conducted by Musa *et al.* [5] suspending a particle containing UWS at the end of a quartz fiber. A comparison of measured particle size evolution with calculated values showed that the fiber significantly influences the heat transfer [6]. It conducts heat to the particle's core and increases its surface.

Musa *et al.* investigated particles containing UWS (concentration of 30% by weight) with initial sizes from 2.36 to 2.95 mm at elevated temperatures from 473 to 773 K. Formation of an unspecified solid white substance during particle lifetime is reported. For 473 and 573 K the substance was left after evaporation at the fiber. For 673 and 773 K the solid turned into a sticky substance before complete decomposition. Birkhold *et al.* [1] concludes that due to the large particle sizes and long lifetime secondary chemical products e.g. cyanuric acid are formed. Thus, for smaller particles and short lifetime as present in aftertreatment systems such products are excluded.

An experimental validation of evaporation and decomposition models on single particles containing UWS of relevant sizes is currently not available to our knowledge. In the following existing crystallisation models are discussed. Afterwards an advanced particle evaporation model is proposed and validated as a first step by experiments with stagnant particles under ambient conditions. To overcome the drawback of a suspension an acoustic levitator is used for particles containing UWS.

Crystallisation Models

At first the basic phenomenon of particle crystallisation is revealed before discussing different models. For this purpose a similar setup as Musa *et al.* [5] is used in the present work for preliminary investigations. The dissolution of urea is depicted in Fig. 1 under ambient conditions. At the beginning urea is completely in solution. The backlight of the microscope and the suspension are clearly visible through the liquid particle (a). After dissolution a crust appears on the surface, which is of irregular shape due to the crystallisation of urea. The core region is still liquid as indicated by the transparency of the particle (b). During evaporation of UWS enrichment

* Corresponding author: sinisa.kontin@kit.edu

of the urea and finally saturation occur inside the particle. The solubility of urea is illustrated in a binary mixture phase diagram in Fig. 2 [7, 8].

Several authors investigated particle crystallisation during a spray drying process. Crystallisation at the particle surface is modelled via formation of a solid crust around the particle which results in a porous layer permeable by water as proposed previously [9, 10]. According to former investigations the main resistance for the heat transfer consists in the gaseous boundary layer around the particle. The strongest resistance to mass transfer is the solid crust. Thus, a homogenous temperature inside the particle can be assumed.

As consequence, the crust is mainly influencing the evaporating mass flow rate

$$\dot{m} = \pi \cdot d \cdot \rho_{gas,ref} \cdot D_{s,ref} \cdot \ln(1 + B_M) \cdot Sh \cdot \phi \ . \tag{1}$$

Where d is the particle diameter, $\rho_{gas,ref}$ the reference gas density, $D_{s,ref}$ the binary diffusion coefficient, B_M the Spalding transfer number and Sh the Sherwood number. Within the transfer number B_M the decreasing water saturation vapour pressure at the surface is considered according to Raoult's law for binary mixtures in agreement with values found in literature [1, 11]. In Eq. (1) the well known film-model [12] is modified by Reinhold [10] introducing the mass flow reduction coefficient

$$\phi = 1 - Y_{sol}, \tag{2}$$

which simply depends on the mass fraction of the solid phase inside the particle Y_{sol}. For the subsequent evaporation process, the precipitation of the solute is accounted for by a mass balance. An oversaturation inside the liquid phase is avoided by an increasing mass fraction Y_{sol} of the inert solid phase inside the particle. For numerical stability reasons Reinhold further proposes the coefficient as

$$\phi = 1 - Y_{sol}^2 \cdot (3 - 2 \cdot Y_{sol}) \ . \tag{3}$$

In general the reduction coefficient function depends on the growth of the solid crust and its properties such as layer thickness and permeability. Even for well studied substances the kinetic properties of the crystal growth are difficult to access [10].

A comprehensive literature review on the crystallisation of urea is given by Grünwald [13]. Most of the literature is focussed on small oversaturation leading to a relatively slow urea crystallisation. For conditions in exhaust aftertreatment systems the oversaturation is significantly higher. Therefore, Grünwald points out that it cannot be excluded that crystallisation occurs within the particle lifetime. In his work the mass flow reduction due to a crust is theoretically investigated. It is modelled by applying a constant reduction coefficient immediately after saturation. The dynamic behaviour of the growing crust is neglected without considering an increasing solid mass. Results for between 0.4 and 1 (no reduction) under ambient temperatures from 523 to 723 K show no significant impact. Instead of an experimental validation his model is compared to numerical data from Birkhold [1]. Therefore, an experimental validation of the model especially focusing on the transition from evaporation to decomposition is lacking.

One cannot study the governing chemical kinetics without incorporating physical resistances against mass transfer [14]. A mass transfer resistance depending on a growing crust is investigated for particles containing UWS for the first time in this work. For this purpose an advanced dynamic reduction coefficient is introduced consecutively.

Details of particle Evaporation

Biot numbers Bi calculated in this work for UWS approve small estimated values around 10^{-2} under relevant conditions. Therefore, the heat conductivity λ_d inside the particle compensates the heat transfer α at the surface. The assumption of a homogenous temperature profile inside the particle without spatial gradients seems to be valid. Therefore, the used model is based on the RM model as proposed by Birkhold [1].

In the presented advanced model, the dynamic behaviour of the growing crust is considered by

$$\phi_n = [1 - Y_{sol}^2 \cdot (3 - 2 \cdot Y_{sol})]^n, \tag{4}$$

which compared to Eq. (3) additionally depends on the exponential parameter n. The parameter n depends on the crystallisation kinetics and the permeability of the crust. The dissolution enthalpy h_{dis} is considered in the energy conservation leading to an increase of the particle temperature.

In the following the calculated evolution of a single evaporating UWS-particle is discussed. The particle and the dry surrounding gaseous phase are stagnant. The initial particle size d_0, temperature T_0 and urea concentration $Y_{u,0}$ by weight are 100 µm, 293 K and 32,5% (as in AdBlue®), respectively. The ambient temperature T_∞ and pressure p_∞ are set to 673 K and 1.0 bar. The dissolution enthalpie h_{dis} and other governing properties are listed in Tab. 1 if not taken from standard literature [15].

The calculations are conducted considering three different cases during evaporation of water and enrichment of urea:

- In the *oversaturated case* urea completely remains in solution, therefore an unlimited oversaturation is possible.
- In the *bounded saturated case* a limited solubility is considered by precipitation of solid crystalline urea out of the liquid phase. This solely influences the saturation pressure according to Raoult's law due to the limited urea concentration in the liquid phase.
- In the *inhibiting crust case* a solid layer is formed at the particle surface during dissolution which reduces the mass transfer. If not indicated differently the parameter n for determining the reduction coefficient is set to 1 (Eq. (2)).

The three cases are compared to a pure water droplet under same initial conditions. First the comparison is focussed on the primary stage of the particle lifetime in which only water evaporates. Afterwards the thermal decomposition of urea is discussed. Finally the evaporation process of single particles is investigated experimentally to determine the unknown reduction coefficient and to quantify the unknown parameter n. The investigations following are conducted under low temperature conditions as a first validation.

Evaporation

In Fig. 3 the evolution of the particle mass m^* which is normalised by the initial mass is shown. The time t^* is normalised by the lifetime of the water droplet ($t_{evap,w}$= 266 ms). The smaller evaporation rate of the UWS indicates the decreased saturation pressures due to the increased urea concentrations. For better comparison the evolution of the three UWS cases is shown in detail in Fig. 3. In the oversaturated case the evaporation takes the longest time. Due to the high urea concentration the saturation vapour pressures decreases most. Therefore, the evaporation rate is the lowest. In the saturated case the evaporation time is reduced. Due to dissolution the concentration in the liquid phase remains lower than for the oversaturated case. Thus, the saturation vapour pressure remains high and the mass transfer is more pronounced. In the case of the inhibiting crust the mass transfer is decreased compared to the bounded saturated case. Therefore, the actual evaporation is inbetween the oversaturated (unlimited soluble) and bounded saturated (limited soluble) case.

In Fig. 5 the corresponding particle temperatures are plotted versus the urea concentration in the liquid phase $Y_{u,liq}$. Conditions where the oversaturated case exceeds the saturation concentration are displayed. Due to the low vapour pressures the highest temperatures occur. In the saturated case the concentration remains lower and constant at around 80% by weight. This leads according to Roult's law to a higher vapour pressure, pronounced mass transfer and lower temperatures. If a crust is established the mass transfer is inhibited leading to a decrease of the released evaporation enthalpy and higher particle temperatures. A combination of the reduced mass transfer and a more pronounced solubility lead to an elevated particle temperature and the melting point of pure urea is reached.

In Fig. 6 the temporal evolution of particle temperature is shown at the end of the evaporation stage in detail. For water the wet bulb temperature is depicted. As described previously, in the case of the inhibiting crust the temperature reaches values between the limiting cases of the oversaturated and bounded saturated mixture. In case of the crust the evaporation time is between the limiting cases as shown previously by the mass decrease in Fig. 3.

Thermal Decomposition

After evaporation of the water, the urea starts to decompose. The decomposition of urea is simply treated like an evaporation process according to Birkhold [6]. The chemical reactions involved are considered to take place immediately in the gaseous boundary layer at the particle surface. Analogue to an evaporation, the disposed reaction enthalpy of the endothermic decomposition causes cooling the particle. Surrounding gas phase properties as e.g. density, heat capacity, etc. are assumed to remain unaffected. In Fig. 7 the saturation vapour pressures are compared between water and urea. The values for urea are calculated according to experimental results by Birkhold [6]

$$p_u = e^{-\frac{24588}{T}+62,419} \quad . \tag{2}$$

In Fig. 8 the evolution of the particle temperature during urea decomposition is plotted. It is assumed that the urea is molten since the particle temperature remains above the melting point of 406 K. In all cases of droplets containing UWS the particle reaches the same equilibrium temperature after heat up. Similar to water evaporation, the transferred heat and enthalpy of decomposition are balanced. Only the heat up stage differs between the three cases.

In Fig. 9 the evolution of the dimensionless surface $d^{*2}=(d/d_0)^2$ is plotted. As expected, the time evolution of the water droplet agrees well with the d^2-law after a short initial time for heat up. Before and after the transition from evaporation to decomposition the surface of UWS particles decreases linearly with nearly constant rates. The decomposition occurs at lower rates than the evaporation of water. It is similar to the evaporation of bicomponent droplets with a less volatile fraction. The higher particle temperature caused by the lower saturation vapour pressures and the higher reaction enthalpy ($h_{th} \approx 3088$ kJ/kg > $h_{evap} \approx 2300$ kJ/kg) are leading to a reduced heat transfer [1, 6].

In summary, if decomposition is accounted for, differences appear only during heat up at the beginning. The differences are attributed to the varying mass transfer rates and temperatures at the end of water evaporation. Mass transfer rates and temperatures are the same during the predominant steady state conditions. Therefore, the start of the decomposition is just delayed and the evolution of size is shifted towards later times.

The particle lifetimes at different ambient temperatures between 473 and 873 K are compared in Tab. 2. The relative differences are referred to the oversaturated case. For lower temperatures the cases resemble more each other due to lower decomposition rates. In general the surface area linearly decreases with two nearly constant rates for water evaporation and urea decomposition. The overall lifetime is dominated more or less by a nearly equal, long decomposition time in all cases. Therefore, the particle lifetime is relatively less influenced by the differences during transition from evaporation to decomposition. This agrees to the remarks made by Grünwald [13]. However, an experimental validation of the behaviour during transition from evaporation to decomposition is still missing.

Experimental Investigation

To overcome the compromising effects of a suspension, in this work an acoustic levitator [16, 17] is used to hold a single particle at a fixed position. Thus, an investigation under ambient conditions with long particle lifetimes without a disturbing suspension is possible. The acoustical levitator is illustrated in Fig. 10. The surrounding humidity is conditioned by blowing nitrogen around the particle with a flow rate small enough to avoid particle displacement. The surrounding humidity is $9 \cdot 10^3$ ppm at a flow rate of 9.5 l/h and a temperature of 298 K. The particles are observed by backlight illumination from a flashlight. The particle size evolution is captured and recorded with high spatial resolution of 0.44 µm/px at a frame rate of 1 Hz using a CCD-camera. A similar setup for measuring drying kinetics is described by Brask *et al.* [18].

Results and Discussion

In Fig. 11 a single particle containing UWS with an initial urea mass fraction of 32.5% and an initial diameter of 442 µm is shown. During the first 35 s (a to b) the particle size decreases and a glare point at the centre is visible. One second later, at 36 s after start (c) the glare point disappears due to formation of the crust and a slight deformation of the particle is observed. The size and shape of the particle remain constant afterwards for at least another 10 min.

A comparison between calculated and measured results for a particle containing distilled water and UWS are shown in Fig. 12. The time evolution of the dimensionless surface d^{*2} is plotted. The initial diameter d_0 is 469 µm. The time t^* is normalised by the extrapolated lifetime of the water particle $t_{evap,w}$ of 197 s.

Since the ambient temperature is moderate the particle heat up is negligible. The surface decreases linearly in case of a pure water droplet. The measured and predicted data are in good agreement.

The measured time evolution of the particle containing UWS differs significantly from the d^2-law. Initially the surface linearly decreases similar to pure water. After crystallisation occurs, as depicted in Fig.11 (c), the measured surface oscillates around a constant mean value due to rotation of the particle in the levitator. Measurement and calculation are stopped at a time t^* of 1.5. The calculated time evolution is plotted for a varying parameter n (Eq. (2)) of 1, 10 and 100. The calculated final particle size d^2 increases with the parameter n because the evaporation rate is inhibited by the crust at an earlier stage. Dedicated reduction coefficients are plotted versus the solid concentration in Fig. 14. For increased values of n the significantly more pronounced reduction of the mass flow rate can be observed. Due to this effect more amount of water is enclosed inside the particle. The behaviour is contrary to that of pure bicomponent liquid droplets where the higher volatile component will evaporate completely [19]. In the case of the highest parameter $n = 100$ the measured and calculated data agree well.

The present study demonstrates that for the evaporation of UWS under low temperatures, the effect of a solid crust has to be considered. The advanced model as proposed is capable to predict the evaporation of water

out of the solution, the precipitation of the solute and formation of a solid crust with a dynamic behaviour. For higher temperatures the impact of oversaturation seems to be negligible. The particle evolution during transition from evaporation to decomposition has to be validated experimentally. Further experimental investigations will focus on the behaviour at elevated temperatures.

Nomenclature

c_p	specific heat capacity [J·kg^{-1}·K^{-1}]
d	particle diameter [m·s^{-2}]
D	binary diffusion coefficient [m^2·s^{-1}]
h	specific enthalpy [J·kg^{-1}]
m	mass [kg]
M	molar mass [kg·mol^{-1}]
n	exponential parameter [-]
u	velocity [m·s^{-1}]
w	atomic diffusion volume [m^3]
Y	concentration by weight [-]

Greek symbols

α	heat transfer coefficient [W·m^{-2}·K^{-1}]
ϕ	mass flow reduction coefficient [-]
λ	heat conductivity [W·m^{-1}·K^{-1}]
η	dynamic viscosity [Pa·s]
ν	kinematic viscosity [m²·s^{-1}]
ρ	density [kg·m^{-3}]

Subscripts

gas	gaseous
liq	liquid
u	urea
uws	urea-water-solution
ref	reference (1/3-rule)
s	surface
sol	solid
vap	vapour
∞	ambient

Dimensionless numbers

$$Bi = \frac{\alpha \cdot d}{2 \cdot \lambda_d}$$ Biot number

$$B_M = \frac{Y_{vap,s} - Y_{vap,\infty}}{1 - Y_{vap,s}}$$ Spalding transfer number

$$Re = \frac{d \cdot u_{rel} \cdot \rho_{gas}}{\eta_{gas,ref}}$$ Reynolds number

$$Sc = \frac{\nu_{gas,ref}}{D_{s,ref}}$$ Schmidt number

$$Sh = 2 + 0{,}552 \cdot \sqrt{Re} \cdot \sqrt[3]{Sc}$$ Sherwood number

References

[1] Birkhold, F., Meingast, U., Wassermann, P. and Deutschmann, O., *Applied Catalysis B: Environmental* 119-127 (2007).
[2] Frössling, N., *Gerlands Beitrag zur Geophysik*, 52:170–216 (1938).
[3] Sirignano, W., *Fluid Dynamics and Transport of Droplets and Sprays,* Cambridge University Press, 1999.
[4] Frohn, A. and Roth, N., *Dynamics of droplets*, Springer, 2000.
[5] Musa, S., Saito, M., Furuhata, T. and Arai, M., *International Conference on Liquid Atomization and Spray Systems*, Kyoto, Japan, August/September 2006, ID ICLASS06-195.
[6] Birkhold, F., *Selektive katalytische Reduktion von Stickoxiden in Kraftfahrzeugen: Untersuchung der Einspritzung von Harnstoffwasserlösung*, Dissertation, Universität Karlsruhe (TH), Shaker, 2007, pp. 30, pp. 36.
[7] BASF, Technical Datasheet *M 6221 d - AdBlue*®, p. 4 (2006).
[8] Terra Industries Inc., Terra Environmental Technologies, *Urea & Urea Solution - Storage, Handling and Dilution*, p. 4 (2006).
[9] Nešić, S. and Vodnik, J., *Chem. Eng. Sc.* 46:527-537 (1991).
[10] Reinhold, M., *Theoretische und experimentelle Untersuchung zur Sprühtrocknung mit Überlagerung chemischer Reaktion*, Dissertation, Technische Universität Clausthal, Shaker, 2001, pp. 48.
[11] Perman, E. and Lovett, T., *Transactions of The Faraday Society*, pp. 1-19 (1926).
[12] Abramzon, B. and Sirignano, W., *Int. J. Heat Mass Transfer* 32:1605-1618 (1989).
[13] Grünwald, J., *Verbesserung der Reduktionsmitteldispersion und -verdunstung in SCR-Abgasanlagen*, Dissertation, Technische Universität München, 2007.
[14] Levenspiel, O., *Chem. Eng. Sc.* 57:4691–4696 (2002).
[15] *VDI Wärmeatlas – 8. Auflage*, Springer, 1997.
[16] Lierke, E., *Acustica - acta acustica* 82:220-237 (1996).
[17] Lierke, E., *Acustica - acta acustica* 88:206-217 (2002).
[18] Brask, A., Ullum, T., Thybo, P. and Andersen, S.K., *International Conference on Multiphase Flow*, Leipzig Germany, July 2007.
[19] Wilms, J., Arndt, S. and Weigand, B., *International Conference on Liquid Atomization and Spray Systems*, Sorrento, Italy, September 2003.
[20] Meessen, J. H., *Ullmann's Agrochemicals*. Wiley-VCH, 2007.
[21] Gucker, F. J. and Ayres, F., *J. Am. Chem. So.*, pp. 2152-3255 (1937).
[22] Gucker, F. J. and Pickard, H., *J. Am. Chem. So.*, pp. 1464-1472 (1940).
[23] Ruehrwein, R. and Huffman, H., *The Heat Capacity, Entropy and Free Energy of Urea*, Thermal Data. XIX., pp. 1759-1761 (1946).
[24] Egan, E. J. and Luff, B., *Heat of Solution, Heat Capacity, and Density of Aqueous Urea Solutions at 25°C*, J. Chem. Eng. Data, pp. 192-194 (1966).
[25] Ferloni, P. and Della Gatta, G., *Heat capacities of urea, N-methylurea, N-ethylurea, N-(n)propylurea, and N-(n)butylurea in the range 200 to 360 K*, Thermochimica Acta, pp. 203-212 (1995).
[26] Hakin, A., Beswick, C. and Duke, M., *J. Chem. Soc., Faraday Trans.*, pp. 207-214 (1996).

Table 1. Correlations for governing properties with sources

Property	Correlation	Reference
Binary diffusion coefficient	$D_{s,ref} = \frac{1.013 \cdot 10^{-3.5} \cdot T_{ref}^{1.75} \cdot (\frac{M_i + M_{air}}{M_i \cdot M_{air}})^{0.5}}{p_\infty \cdot (w_i^{0.333} + w_{air}^{0.33})^2}$	[8]
Density of UWS (liquid)	$\rho_{uws} = 1144.5 + 280 \cdot Y_u - 0.5 \cdot T$	[13]
Density of urea (solid)	$\rho_u = 1396 - 0.208 \cdot T$	[20]
Heat capacity of urea	$c_{p,u} = 4.1147 \cdot T + 291.07$	[21-26]
Dissolution enthalpy of urea	$h_{dis} = 19317 \cdot Y_{u,liq}^2 - 96454 \cdot Y_{u,liq} + 254585$	[24]

Table 2. Calculated particle lifetime for varying ambient temperatures, initial conditions: d_0 = 100 µm, T_0 = 293 K, $Y_{u,0}$ = 32,5%, u_{rel} = 0 m/s, p_∞ = 1.0 bar

Ambient temperature T_∞ [K]	Lifetime t [s] for case			Relative difference [%]
	over-satured	saturated	crust	
473	2.31	2.29	2.30	0.87
573	0.711	0.701	0.709	1.41
673	0.418	0.411	0.417	1.67
773	0.291	0.286	0.292	1.72
873	0.221	0.217	0.221	1.81

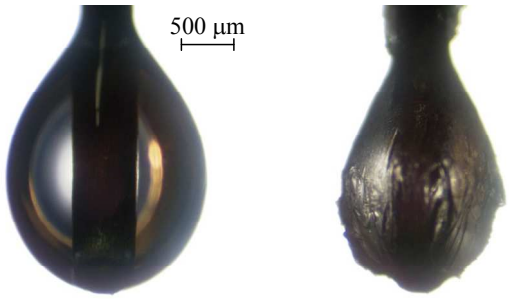

(a) (b)

Figure 1. UWS-particle suspended on a wire in solution (a) and after dissolution (b)

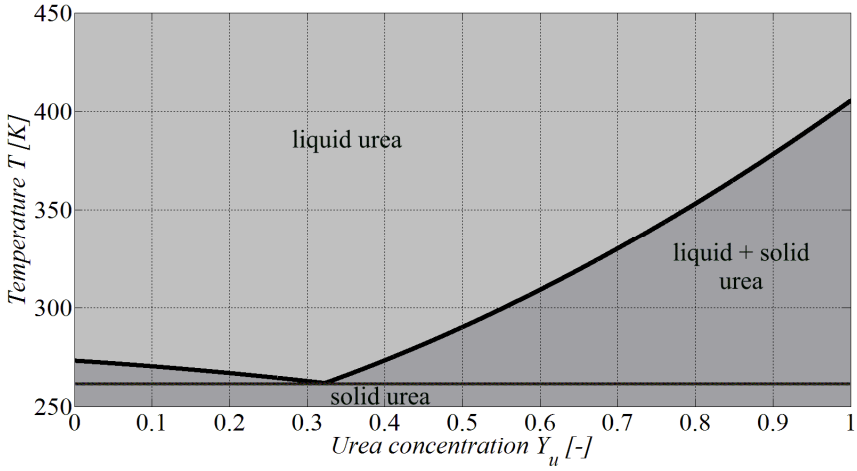

Figure 2. Binary phase diagram of urea-water-mixture [7, 8]

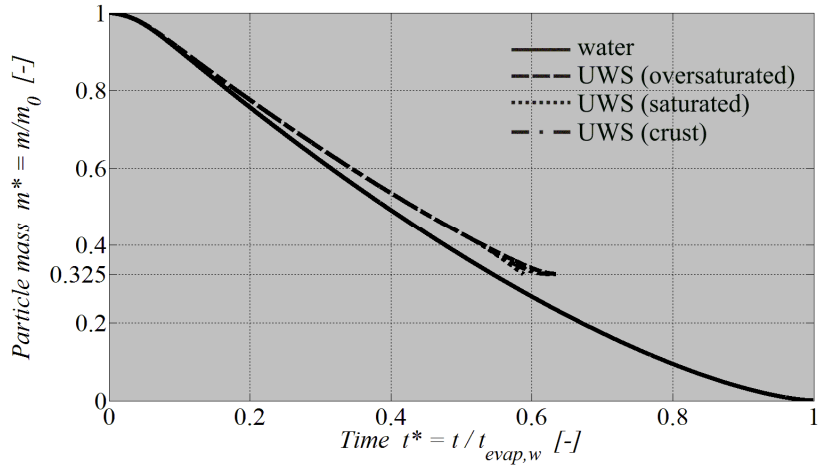

Figure 3. Evolution of particle mass m^*

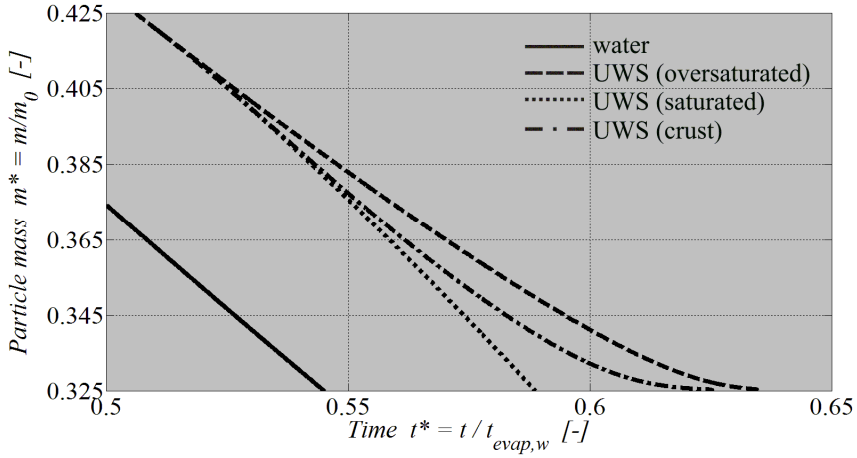

Figure 4. Detailed evolution of particle mass m^*

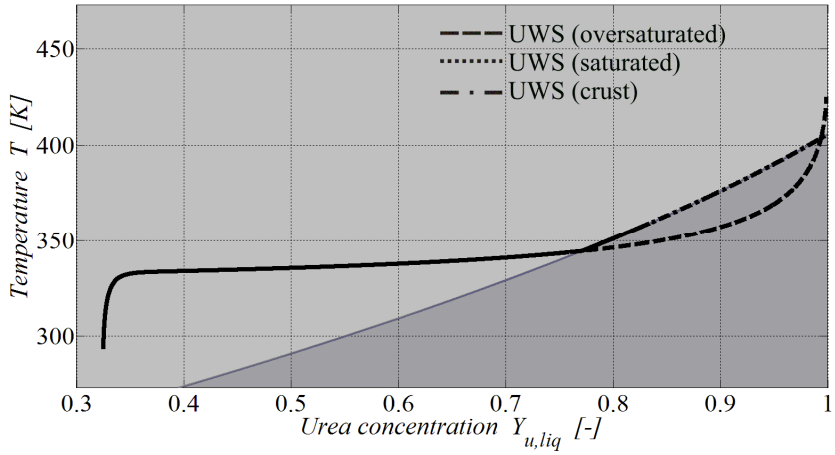

Figure 5. Particle temperature versus urea concentration by weight in the liquid phase, oversaturated conditions indicated by dark region

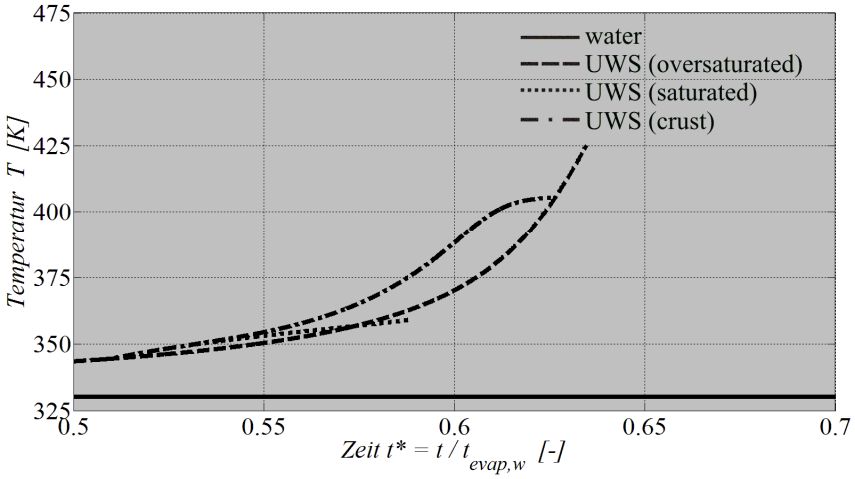

Figure 6. Detailed evolution of particle temperature T

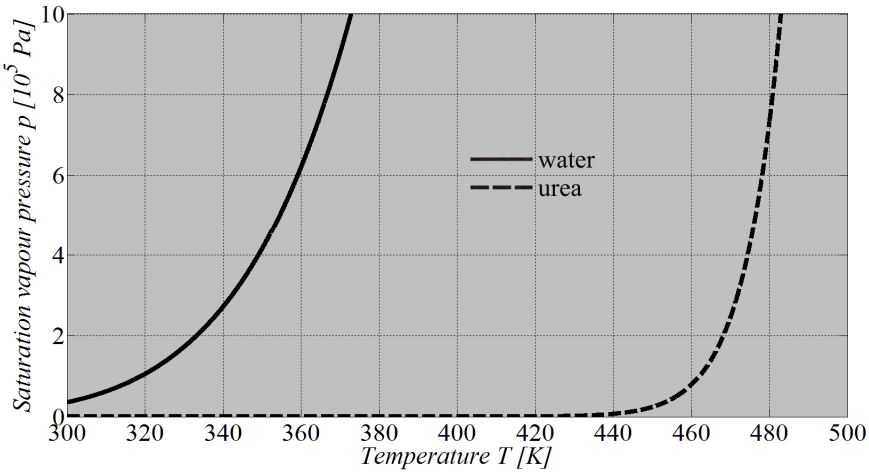

Figure 7. Saturation vapour pressures p of water and urea versus temperature T [6]

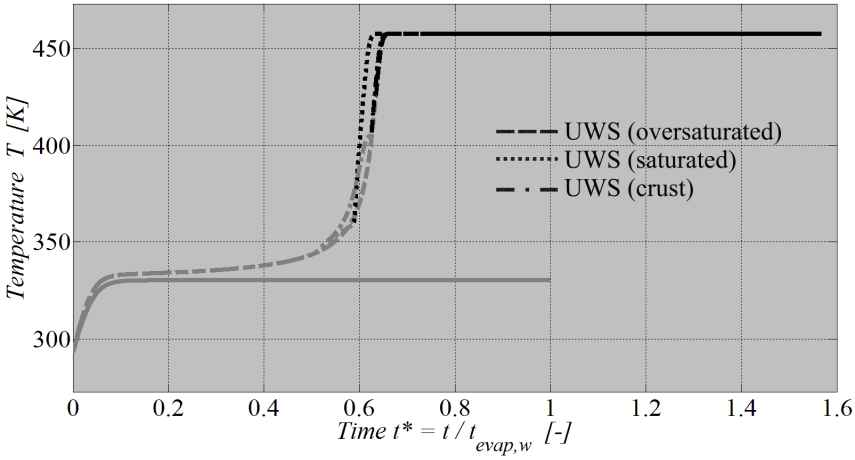

Figure 8. Evolution of particle temperature T during thermal decomposition

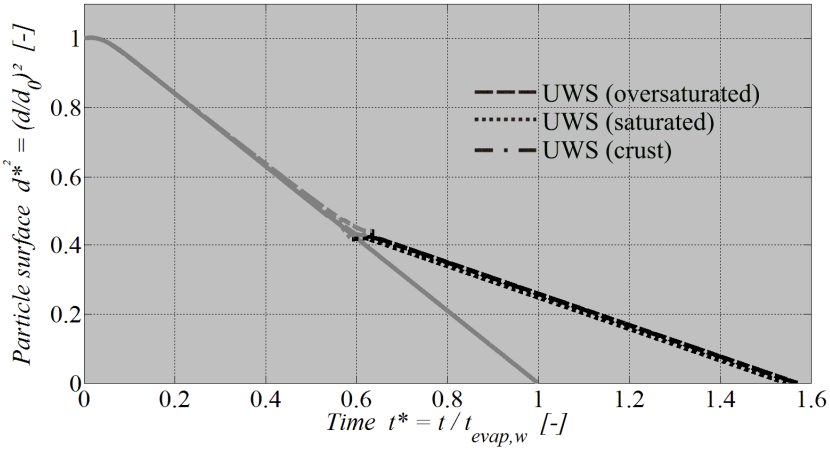

Figure 9. Evolution of surface area d^{*2} during thermal decomposition

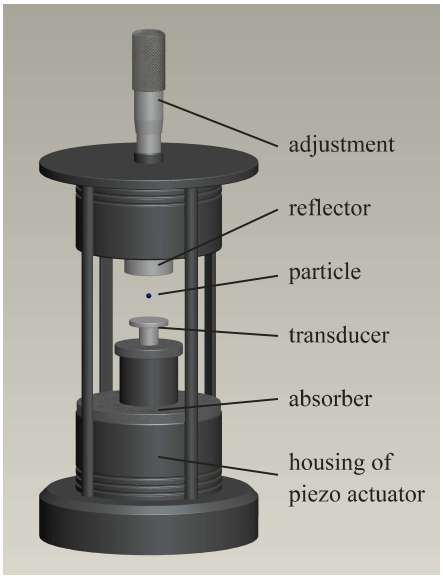

Figure 10. Acoustical levitator (tec5)

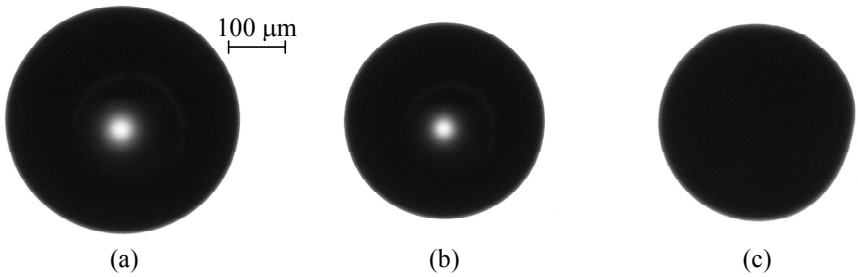

Figure 11. Acoustically levitated particle initially containing UWS

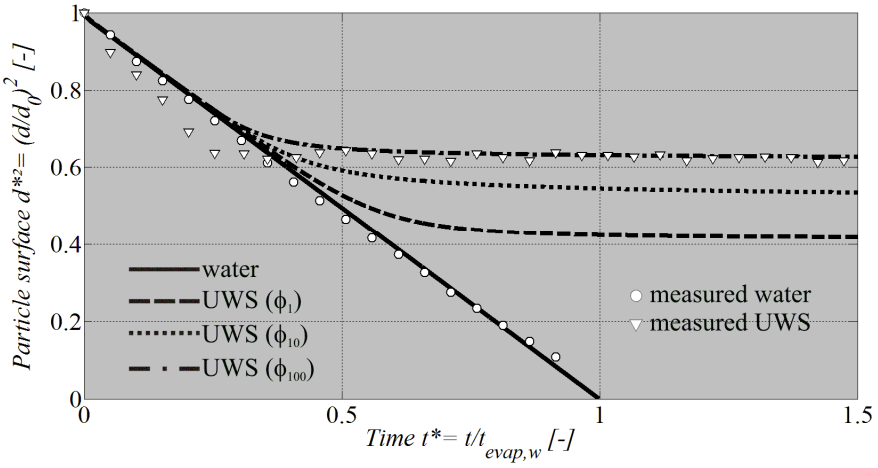

Figure 12. Evolution of surface area d^{*2}, comparison between calculated and experimental results

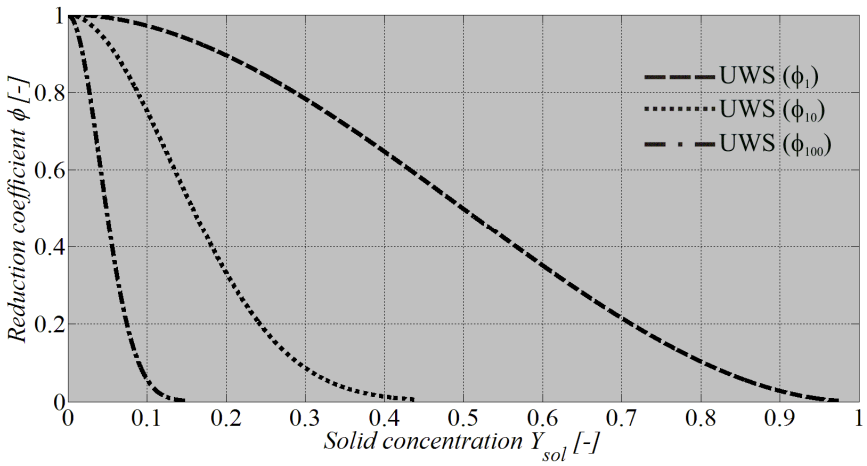

Figure 13. Reduction coefficient ϕ versus solid concentration Y_{sol} by weight